Supplementary Information (SI) for Journal of Materials Chemistry B.

Supporting information

Responsive Nanoprobe for Ratiometric Florescence Detection of Hydroxyl Radical in Macrophage Polarization

Mazen Alanazi,[a] Miaomiao Wu,[a] Jiaxi Yong,[a] Zexi Zhang,[a] Huayue Zhang,[a] Dihua Tian,[a] Run Zhang*[a]

[a] Australian Institute for Bioengineering and Nanotechnology (AIBN), The University of Queensland, St Lucia, QLD 4072, Australia.

E-mail: r.zhang@uq.edu.au

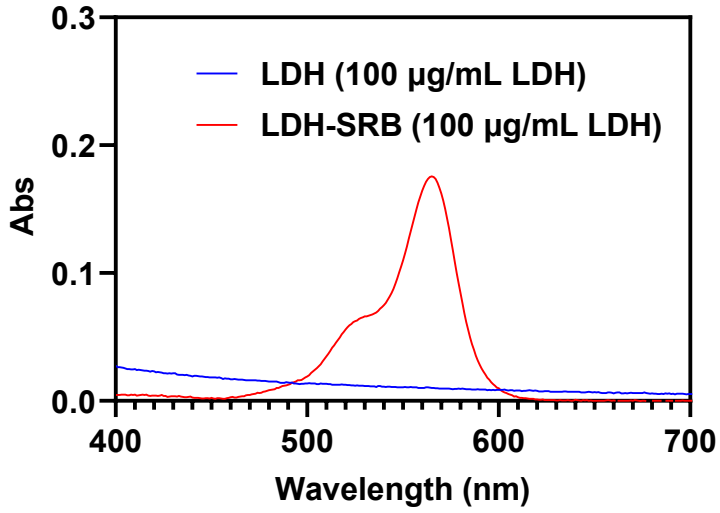

Fig. S1. Absorption spectra of 100 µg/mL of LDH and 100 µg/mL of LDH-SRB.

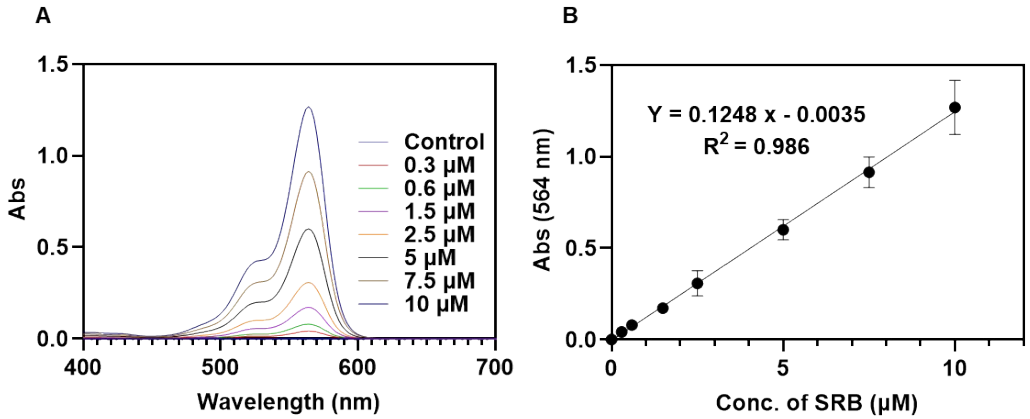

Fig. S2. The standard curve for SRB analysis. (A): The absorption spectra of SRB over different concentrations (0 to 10 μM). (B): The linearity of absorbance at 564 nm against SRB concentrations.

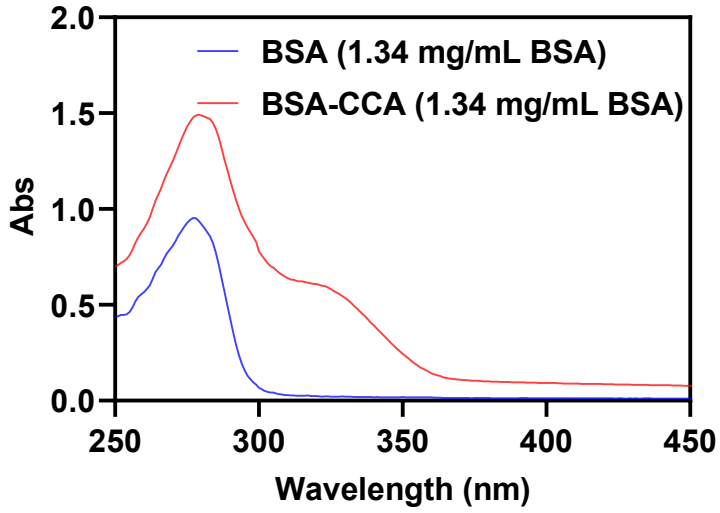

Fig. S3. The absorption spectra of 1.34 mg/mL of BSA and 1.34 mg/mL of BSA-CCA.

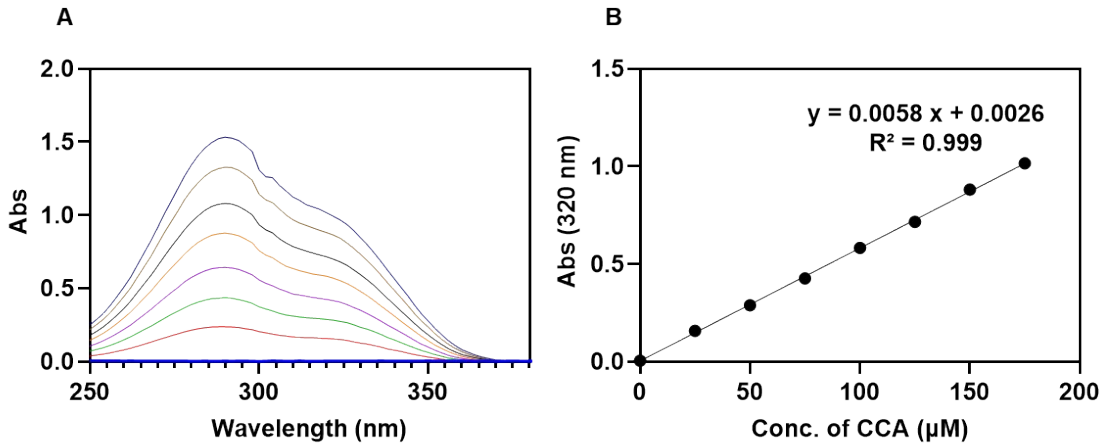

Fig. S4. The standard curve for CCA analysis. (A): The absorption spectra of CCA over different concentrations (0 to 175 μM). (B): The linearity of absorbance at 320 nm against CCA concentrations.

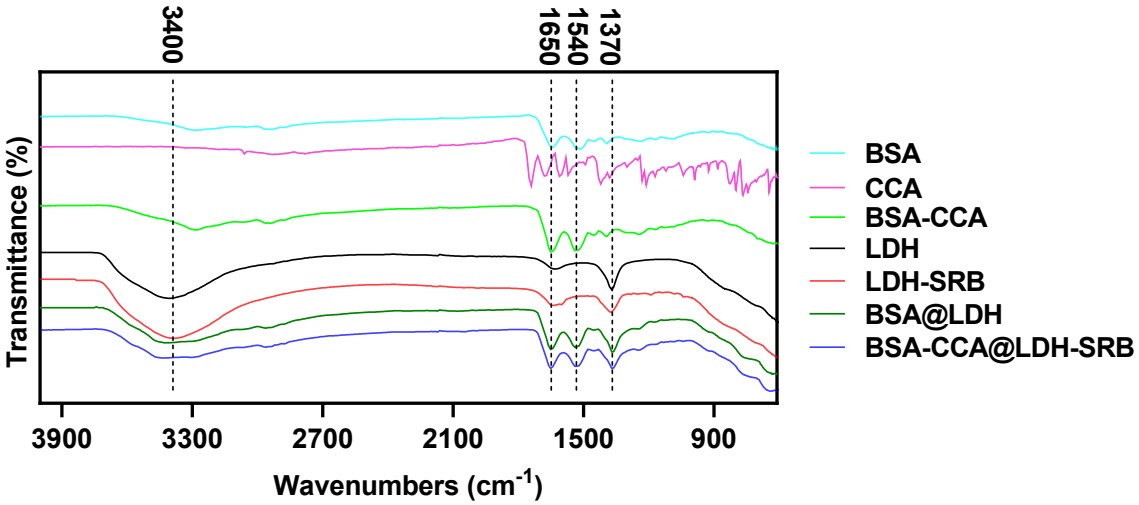

Fig. S5. FTIR spectra of BSA, CCA, BSA-CCA, LDH, LDH-SRB, BSA@LDH, and BSA-CCA@LDH-SRB.

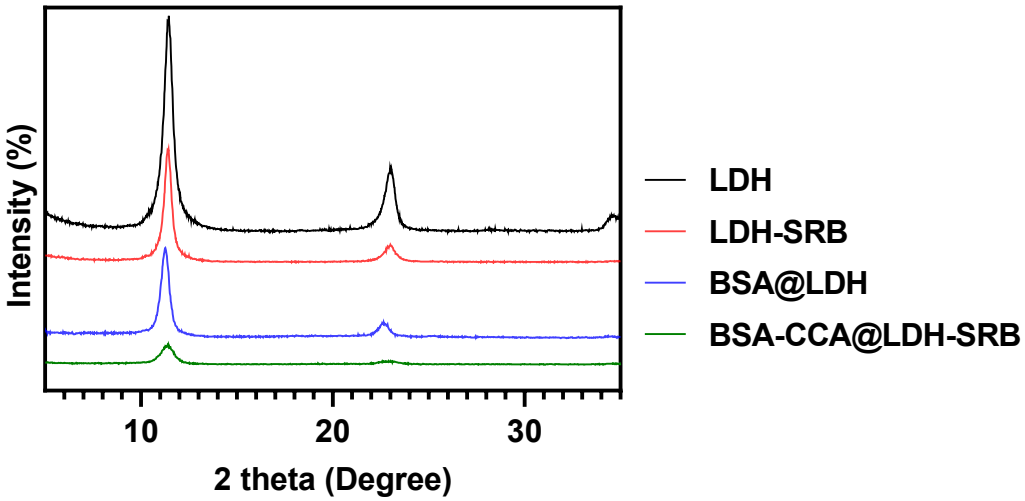

Fig. S6. XRD patterns of LDH, LDH-SRB, BSA@LDH, and BSA-CCA@LDH-SRB.

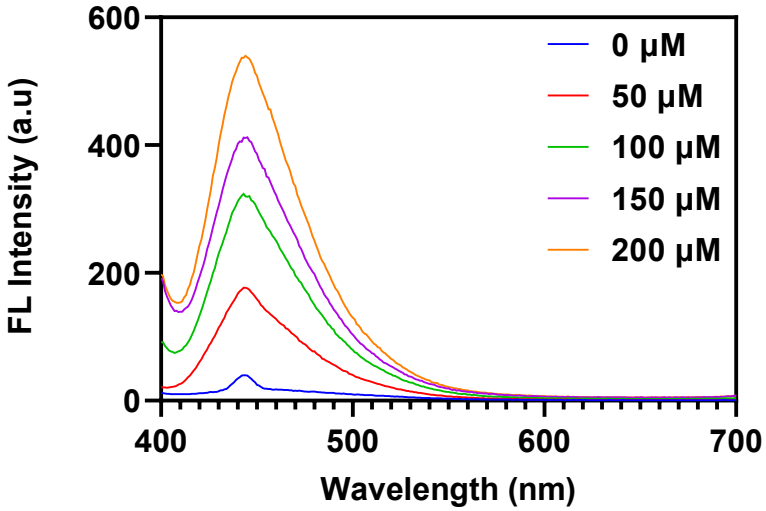

Fig. S7. The fluorescence analysis of BSA-CCA over a range of •OH (0-200 μM) in PBS buffer of pH 7.4.

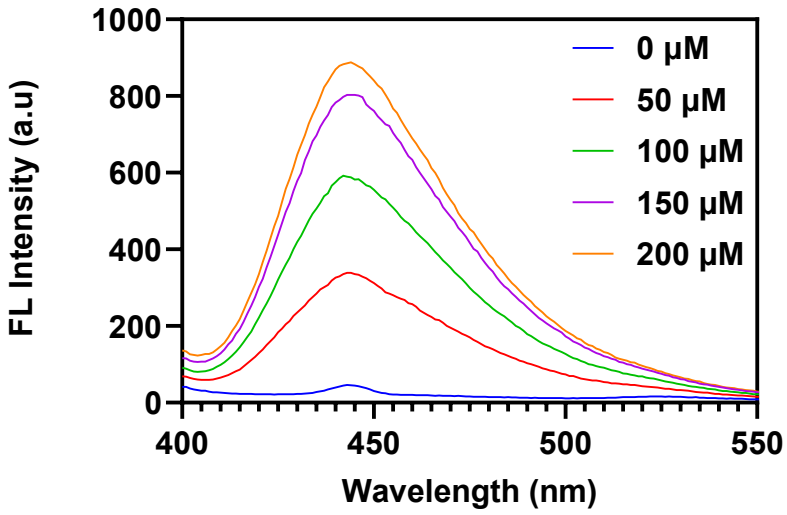

Fig. S8. The fluorescence analysis of BSA-CCA@LDH over a range of •OH (0-200 μM) in PBS buffer of pH 7.4.

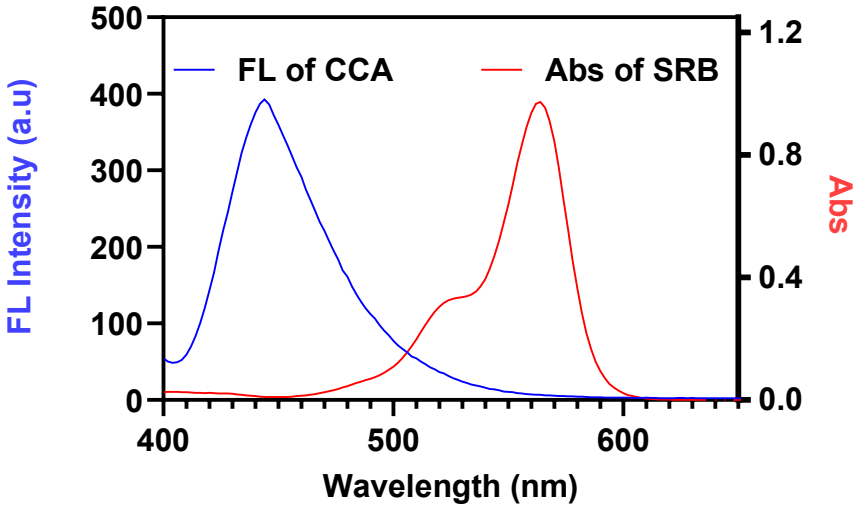

Fig. S9. The spectra of CCA's emission and SRB's absorption.

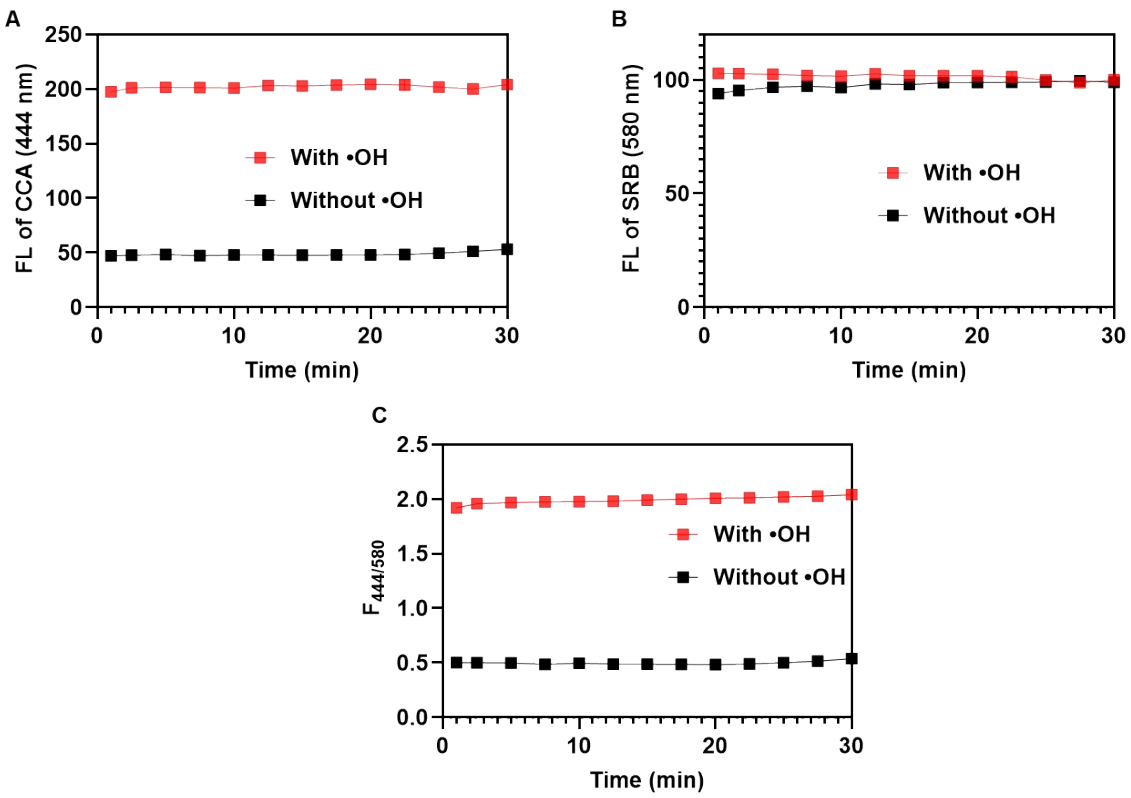

Fig. S10. Time dependent fluorescence analysis of the changes of $F_{444/580}$ ratio in the absence and presence of •OH. (A) The fluorescence analysis (CCA 444 nm) of BSA-CCA@LDH-SRB response over 30 min with and without •OH. (B) The fluorescence analysis (SRB 580 nm) of BSA-CCA@LDH-SRB response over 30 min with and without •OH. (C) Fluorescence of $F_{444/580}$ ratio over 30 min in the presence and absence of •OH.

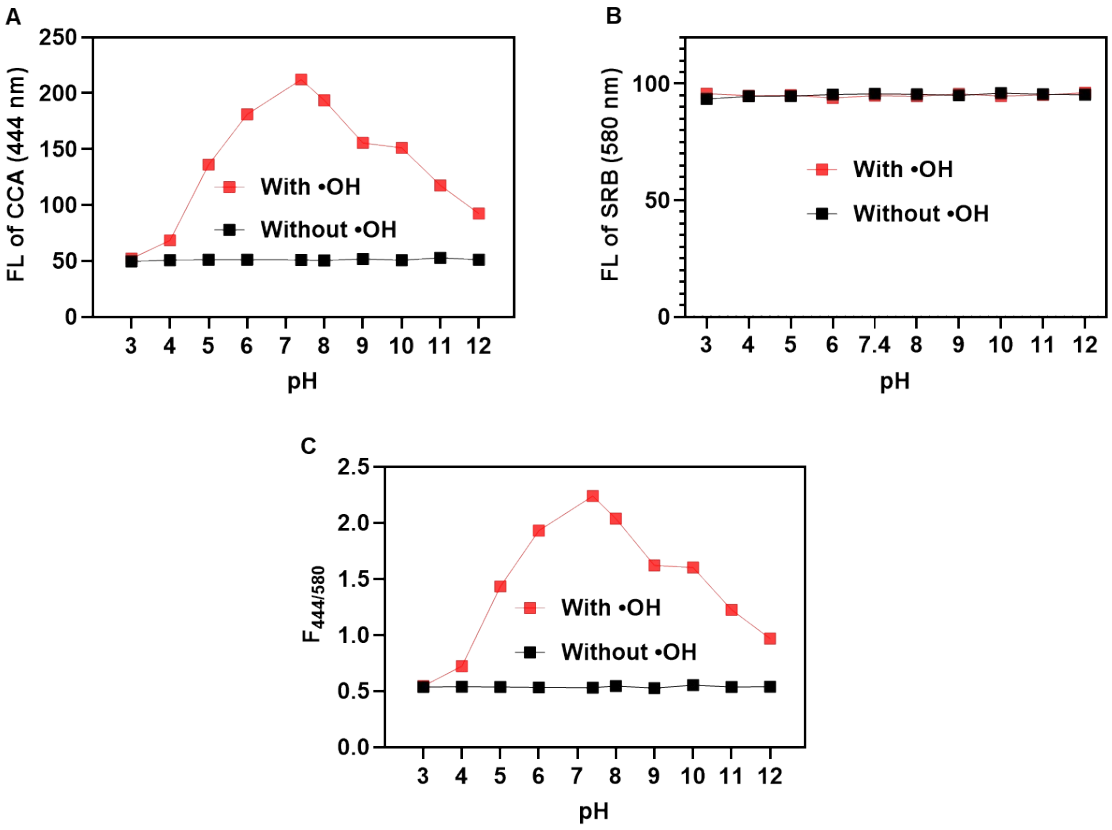

Fig. S11. Fluorescence analysis of the changes of $F_{444/580}$ ratio at different pH. (A) The fluorescence analysis (CCA 444 nm) of BSA-CCA@LDH-SRB response over a wide range of pH with and without •OH. (B) The fluorescence analysis (SRB 580 nm) of BSA-CCA@LDH-SRB response over a wide range of pH with and without •OH. (C) Fluorescence of $F_{444/580}$ ratio over a wide range of pH in the presence and absence of •OH.

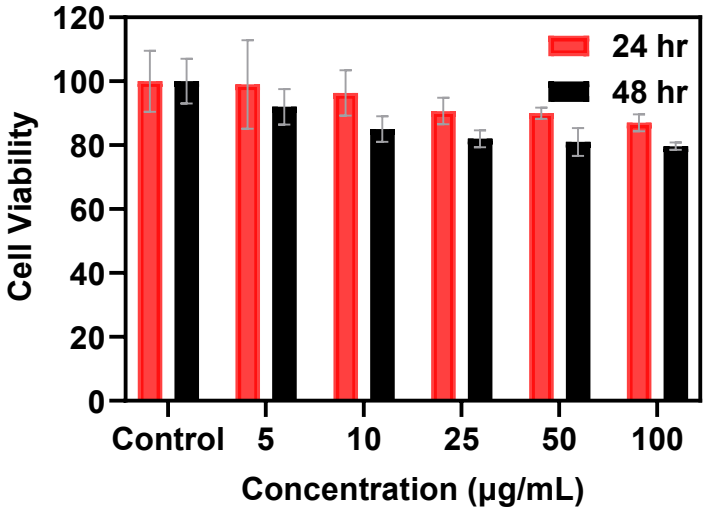

Fig. S12. Viability of RAW246.7 cells incubated with BSA-CCA@LDH-SRB at different concentrations (0 to 100 μg/mL) over 24 and 48 h.

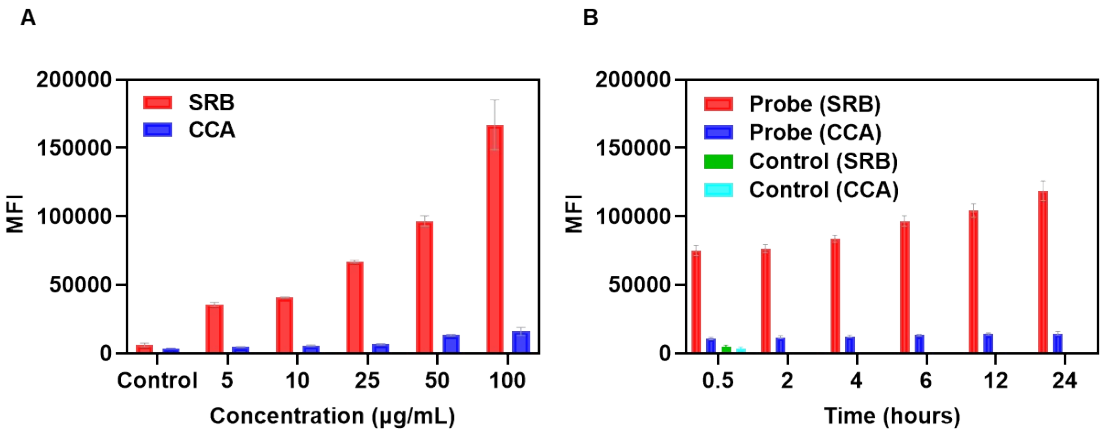

Fig. S13. Cellular internalisation analysis of BSA-CCA@LDH-SRB in RAW246.7. (A) The cellular uptake of BSA-CCA@LDH-SRB over various concentrations in RAW 246.7 cells. (B) The time-dependent cellular uptake of 50 µg/mL BSA-CCA@LDH-SRB in RAW 246.7 cells.

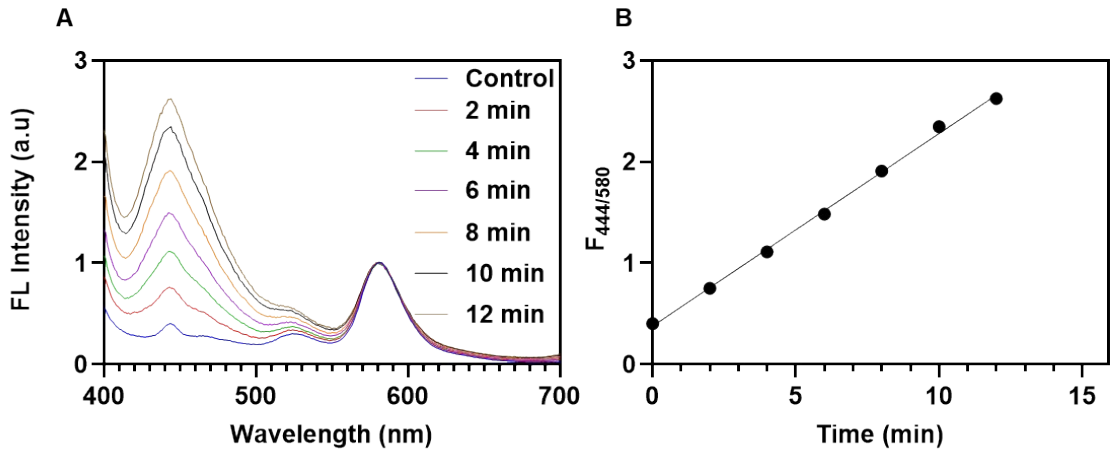

Fig. S14. The fluorescence analysis ($F_{444/580}$ ratio) of BSA-CCA@LDH-SRB response to ultrasound (US) treatment in PBS buffer of pH 7.4.

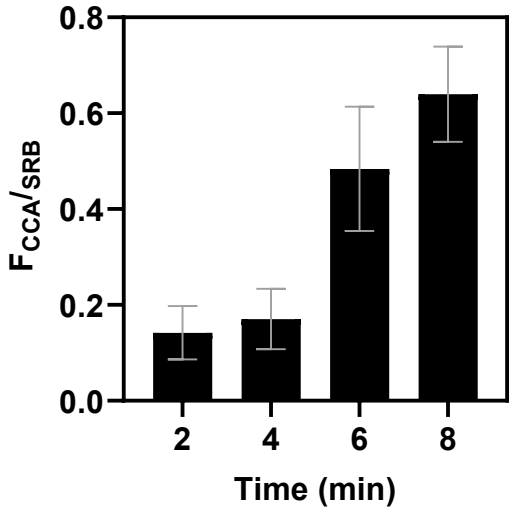

Fig. S15. The MFI of RAW264.7 cells incubated with BSA-CCA@LDH-SRB for US treatment over different time points (0 to 8 min).

Table. S1. Responsive nanoprobes for detection of •OH.

Probe	LOD	Em (nm)	Fluorescence signal type	Application	Ref
BSA-CCA@LDH-SRB	12.6 nM	444, 580	Ratiometric	Detection of •OH in macrophage polarisation	This work
CONER	0.73 μM	450, 528	Ratiometric	Detection of •OH in MCF-7 cells	[1]
ROX@SiO_2	1.65 μM	455, 620	Ratiometric	Detection of •OH in HeLa cells	[2]
CCA@TPP@CDs	70 nM	451, 577	Ratiometric	Detection of •OH in RAW 264.7 cells	[3]
TPA@CDs	0.25 μM	326, 423	Ratiometric	Detection of •OH in environmental samples	[4]
AuNC@HPF	0.68 μM	515, 637	Ratiometric	Detection of •OH in HeLa cells	[5]
UCNP-ICG	100 pM	654, 540	Ratiometric	Detection of •OH in live hepatocyte	[6]
Brite/DEVD@LMWCNP	NA	663	Turn-On	Detection of •OH during drug-induced kidney injury	[7]
TPA@GQDs	12 nM	430	Turn-On	Detection of •OH in HeLa cells	[8]
AuNPs	NA	520	Turn-On	Detection of •OH in L-02 cells	[9]
FAM-DNA-AuNPs	2.4 nM	517	Turn-On	Detection of •OH in macrophages and HepG2 cells	[10]
mOG-SWUCNPs	1.2 fM	478	Turn-On	Detection of •OH in HeLa cells and liver tissues	[11]

References

[1] G. M. Ganea, P. E. Kolic, B. El-Zahab, I. M. Warner, *Analytical chemistry* **2011**, *83*, 2576-2581.

[2] S. Liu, J. Zhao, K. Zhang, L. Yang, M. Sun, H. Yu, Y. Yan, Y. Zhang, L. Wu, S. Wang, *Analyst* **2016**, *141*, 2296-2302.

[3] D. Zhou, H. Huang, Y. Wang, Y. Wang, Z. Hu, X. Li, *Journal of Materials Chemistry B* **2019**, *7*, 3737-3744.

[4] H. Wang, T. Fu, M. Ai, J. Liu, *Analytical and Bioanalytical Chemistry* **2022**, *414*, 6735-6741.

[5] M. Zhuang, C. Ding, A. Zhu, Y. Tian, *Analytical chemistry* **2014**, *86*, 1829-1836.

[6] Q. Guo, Y. Liu, Q. Jia, G. Zhang, H. Fan, L. Liu, J. Zhou, *Analytical chemistry* **2017**, *89*, 4986-4993.

[7] Y. Tong, X. Huang, M. Lu, B.-Y. Yu, J. Tian, *Analytical chemistry* **2018**, *90*, 3556-3562.

[8] X. Hai, Z. Guo, X. Lin, X. Chen, J. Wang, *ACS applied materials & interfaces* **2018**, *10*, 5853-5861.

[9] B. Ma, M. Lu, B.-Y. Yu, J. Tian, *RSC advances* **2018**, *8*, 22062-22068.

[10] B. Tang, N. Zhang, Z. Chen, K. Xu, L. Zhuo, L. An, G. Yang, *Chemistry–A European Journal* **2008**, *14*, 522-528.

[11] Z. Li, T. Liang, S. Lv, Q. Zhuang, Z. Liu, *Journal of the American Chemical Society* **2015**, *137*, 11179-11185.